

LETTERS

Crystal structure of the heterotrimer core of *Saccharomyces cerevisiae* AMPK homologue SNF1

Gabriele A. Amodeo^{1*}, Michael J. Rudolph^{1*} & Liang Tong¹

AMP-activated protein kinase (AMPK) is a central regulator of energy homeostasis in mammals and is an attractive target for drug discovery against diabetes, obesity and other diseases^{1–5}. The AMPK homologue in *Saccharomyces cerevisiae*, known as SNF1, is essential for responses to glucose starvation as well as for other cellular processes, although SNF1 seems to be activated by a ligand other than AMP^{1,6–8}. Here we report the crystal structure at 2.6 Å resolution of the heterotrimer core of SNF1. The ligand-binding site in the γ -subunit (Snf4) has clear structural differences from that of the *Schizosaccharomyces pombe* enzyme⁹, although our crystallographic data indicate that AMP can also bind to Snf4. The glycogen-binding domain in the β -subunit (Sip2) interacts with Snf4 in the heterotrimer but should still be able to bind carbohydrates^{10–13}. Our structure is supported by a large body of biochemical and genetic data on this complex^{1,6–8,14–18}. Most significantly, the structure reveals that part of the regulatory sequence in the α -subunit (Snf1)^{15,16,18,19} is sequestered by Snf4, demonstrating a direct interaction between the α - and γ -subunits and indicating that our structure may represent the heterotrimer core of SNF1 in its activated state.

Most AMPKs (including SNF1) are heterotrimeric enzymes, consisting of one catalytic subunit (α) and two regulatory subunits (β and γ ; Fig. 1a, and see Supplementary Figs 1–3 for alignment of their sequences). The Ser/Thr protein kinase domain is located at the amino terminus of the α -subunit^{20,21}, and a regulatory sequence helps to control the activity of this enzyme^{15,16,18,19}. The β -subunit contains a glycogen-binding domain (GBD) that may target the heterotrimer to glycogen storage sites^{10,11,13}. The γ -subunit contains two tandem pairs of the cystathionine- β -synthase (CBS) motifs, each of which is also known as a Bateman domain^{22,23}. Binding of AMP or ATP to the γ -subunit regulates the activity of the protein kinase domain in the α -subunit. This is supported by the observations that mutations in the γ -subunit can affect nucleotide binding and cause diseases^{1,2,24,25}.

We have determined the crystal structure of the heterotrimer core of *S. cerevisiae* SNF1 at 2.6 Å resolution. The expression construct contains residues 398–633 of the α -subunit (Snf1, lacking the protein kinase domain), residues 154–415 of the β -subunit (Sip2), and the entire γ -subunit (Snf4, residues 1–322; Fig. 1a). (We are following the convention of using SNF1 to indicate the heterotrimer and using Snf1 to indicate the α -subunit⁶.) The three subunits were expressed together in *Escherichia coli* from a single plasmid, and they purified together through Ni²⁺-affinity and gel-filtration chromatography (Supplementary Fig. 4). The refined structure has excellent agreement with the crystallographic data and the expected bond lengths, bond angles, and other geometric parameters (Supplementary Table 1). Most of the residues (82%) are in the most favoured region of the Ramachandran plot.

The structure shows that there are intimate interactions among the three subunits in the heterotrimer, as observed previously with the *S. pombe* enzyme⁹. A central component of this heterotrimer interface is an eight-stranded, mostly antiparallel β -sheet, formed with four strands from Snf1 (residues 531–586), three strands from Sip2 (from the extreme C-terminal region, residues 375–412) and one strand from Snf4 (residues 38–45, the first β -strand of CBS1, β 1A; Fig. 1b and Supplementary Fig. 5). The hydrophobic core of this interface is located between the β -sheet and two helices from Snf1 (residues 515–529 and 612–630). The two neighbouring strands of the β -sheets in Snf1 and Sip2 share only a few hydrogen bonds at one end, and are splayed apart from each other at the other end (Fig. 1b and Supplementary Fig. 5). Residues 504–511 of Snf1 form two small β -strands (shown in red in Fig. 1b, because they are part of the regulatory sequence) that interact with the open ends of the two β -sheets, providing further stabilization of the heterotrimer. Additional interactions between the three subunits are mediated by the β -hairpin structures in the β -sheets of the Bateman1 domain of Snf4 (Fig. 1b and Supplementary Fig. 5). Our structure of the heterotrimer core is supported by a large body of biochemical and genetic studies on SNF1 (refs 6, 14, 15, 17).

We have observed new structural features for the AMPK heterotrimer from our studies, because the expression construct for the SNF1 complex contains about 100 more residues for the α -subunit and 160 more residues for the β -subunit than those of the *S. pombe* enzyme structure⁹. Most importantly, the structure shows that residues 460–495 of Snf1 have well-defined interactions with Snf4, including an antiparallel β -sheet between residues 467–469 of Snf1 and residues 270–275 of Snf4 (the first β -strand of CBS4, β 4A; Fig. 1b and Supplementary Fig. 6). This demonstrates a direct interaction between the α - and γ -subunits in SNF1, which is supported by earlier biochemical and genetic data¹⁵. The L470S mutation in Snf1, which can disrupt this interaction¹⁵, is located in the interface between Snf1 and Snf4 in our structure (Fig. 1b and Supplementary Fig. 6). This direct interaction has significant implications for the regulation of the protein kinase activity of SNF1, because residues 460–495 are part of the regulatory sequence of Snf1 (see below).

Another new feature of our structure is the presence of the GBD in the β -subunit (Sip2; Fig. 1a). The GBD has close interactions with the rest of the heterotrimer, primarily with the N-terminal region (the first helix and the following loop) and a helix (α 2B) in CBS2 of Snf4 (Fig. 1b). Residues in the hydrophobic core of this interface are mostly conserved, indicating that the GBD may also have a similar conformation in mammalian AMPKs. The putative binding site for carbohydrates, as revealed by the binding of β -cyclodextrin¹⁰, is exposed to the solvent and should be available for binding ligands in this complex (Fig. 1b).

¹Department of Biological Sciences, Columbia University, New York, New York 10027, USA.

*These authors contributed equally to this work.

Besides these new structural features, the overall structure of the *S. cerevisiae* SNF1 heterotrimer is similar to that of the *S. pombe* AMPK reported recently (Fig. 1c)⁹. The root mean squared distance for 280 equivalent C α atoms in the γ -subunits of the two structures is 1.4 Å, and that for 142 equivalent C α atoms in the α - and β -subunits is 1.2 Å. However, there is a significant difference in the positions of the α - and β -subunits relative to the γ -subunit in the two structures (Fig. 1c), corresponding to a rotation of about 12°. Whereas all the loops in the *S. pombe* structure are defined, many of the loops in the structures of the Snf1 and Sip2 subunits are missing in the current SNF1 structure as a result of disorder (Fig. 1b).

The two Bateman domains in the γ -subunit are arranged in a head-to-head fashion, with an extensive, hydrophobic interface between them formed by two helices (α A and α B) from each CBS motif (Fig. 2a). (The secondary structure elements in the CBS motifs are named in accordance with the convention devised previously²⁶.) The first CBS motif is much larger than the second one in each Bateman domain (Fig. 1a), because it contains an extra crossover connection and an extra helix (α C; Fig. 2a)²⁶. Overall, the γ -subunit has the shape of a disc, with a diameter of about 55 Å and a thickness of about 30 Å.

Earlier structural studies of the Bateman2 domain alone, from *S. cerevisiae*²⁶ and from humans²⁷, showed a homodimer, and the overall shape of this dimer is also a disc (Fig. 2b). However, the two monomers are arranged in a head-to-tail fashion, even though the same two helices (α A and α B) are used for the formation of the dimer. The structure of the Bateman2 domain in this homodimer is very different from that in full-length Snf4, with a root mean squared distance of 1.3 Å for 113 equivalent C α atoms (Fig. 2c). The largest

structural differences are for the two helices (α A and α B) that mediate the dimeric association. Nonetheless, the human Bateman2 domain homodimer can bind two AMP molecules, obeying the two-fold symmetry of the dimer²⁷.

We included 1 mM AMP in the crystallization solution but did not observe any electron density for it in this crystal. A comparison of our structure with that of *S. pombe* AMPK in complex with AMP⁹ reveals that there are main-chain and side-chain differences between them in the AMP-binding site (Fig. 3). The phosphate group of AMP interacts with the side chains of three Arg residues in *S. pombe* AMPK⁹ (Fig. 3). One of them is equivalent to Arg 143 in Snf4, whose side chain clashes with the AMP molecule in the *S. pombe* enzyme (Fig. 3). The second Arg residue is equivalent to Gly 145 in Snf4 (Fig. 3) and a His residue in the mammalian γ -subunits (Supplementary Fig. 3). Mutation of this His residue to Gly is sufficient to make the mammalian enzyme insensitive to AMP²⁸. Mutation of this His residue to Arg in the γ 2-subunit is linked to the Wolff–Parkinson–White syndrome and reduces the affinity for the nucleotide²⁴. The third Arg residue, Arg 294 in Snf4, also corresponds to the site of a disease-causing mutation in mammalian γ -subunits, equivalent to Val 63 and Thr 166 in Snf4, are located in a pocket on the opposite face of the Snf4 disc (Fig. 3).

Crystallographic analysis on diffraction data at 3.3 Å resolution collected on another crystal, grown under the same conditions but with large differences in unit cell parameters, revealed the presence of an AMP molecule in Snf4 (Supplementary Fig. 7), at essentially the same position as that observed in the *S. pombe* enzyme (Fig. 3). The

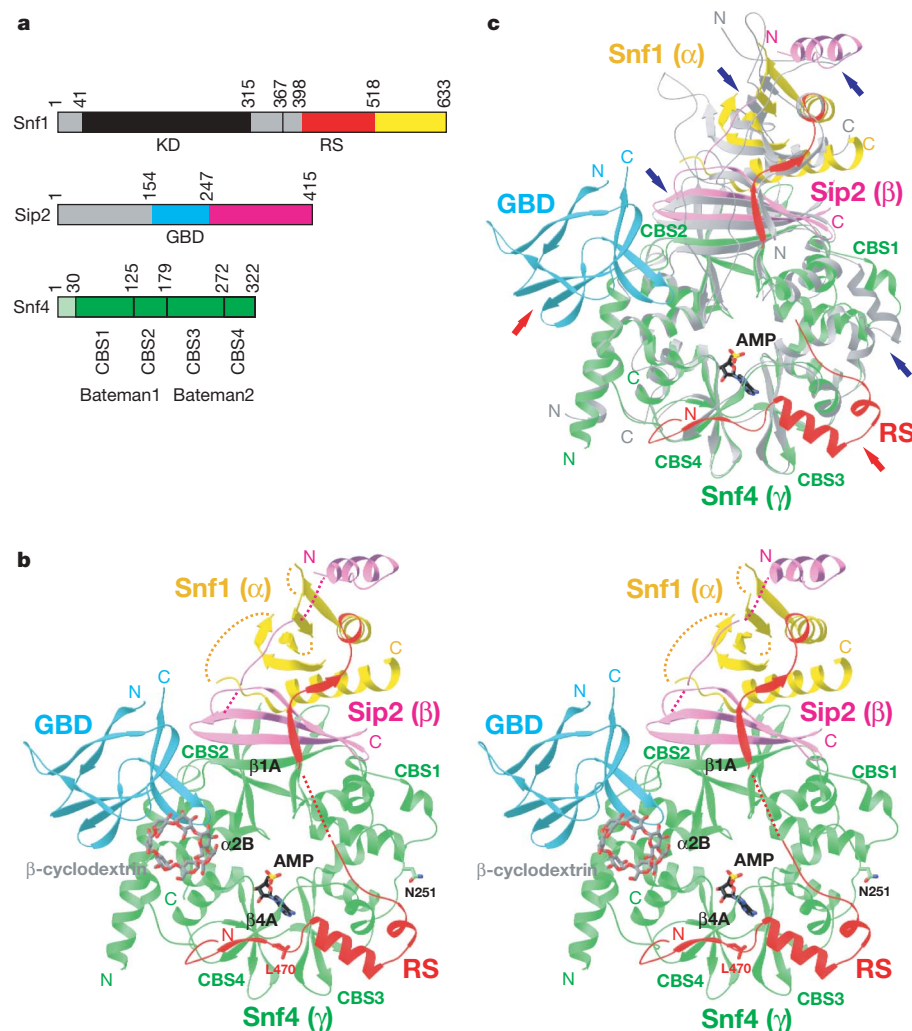


Figure 1 | Structure of the heterotrimer core of *S. cerevisiae* SNF1. **a**, Domain organization of SNF1 subunits. Residues that are included in the co-expression construct are shown in colour, and the others are shown in grey or black. KD, protein kinase domain; RS, regulatory sequence. **b**, Schematic representation (stereo view) of the heterotrimer core of SNF1. The regulatory sequence of the α -subunit (Snf1) is shown in red and the rest is in yellow; the GBD of the β -subunit (Sip2) is shown in cyan and the rest is in magenta; and the γ -subunit (Snf4) is shown in green. The positions of AMP (stick model in black), as observed from our studies and in the *S. pombe* enzyme⁹, as well as that of β -cyclodextrin (in grey) as bound in the rat GBD¹⁰, are shown for reference. **c**, Superposition of the structures of *S. cerevisiae* SNF1 (coloured as in **b**) and *S. pombe* AMPK (in grey)⁹. The superposition is based on the γ -subunits only. Red arrows point to new features in the SNF1 structure, and blue arrows point to differences between the two structures. Produced with Ribbons³⁰.

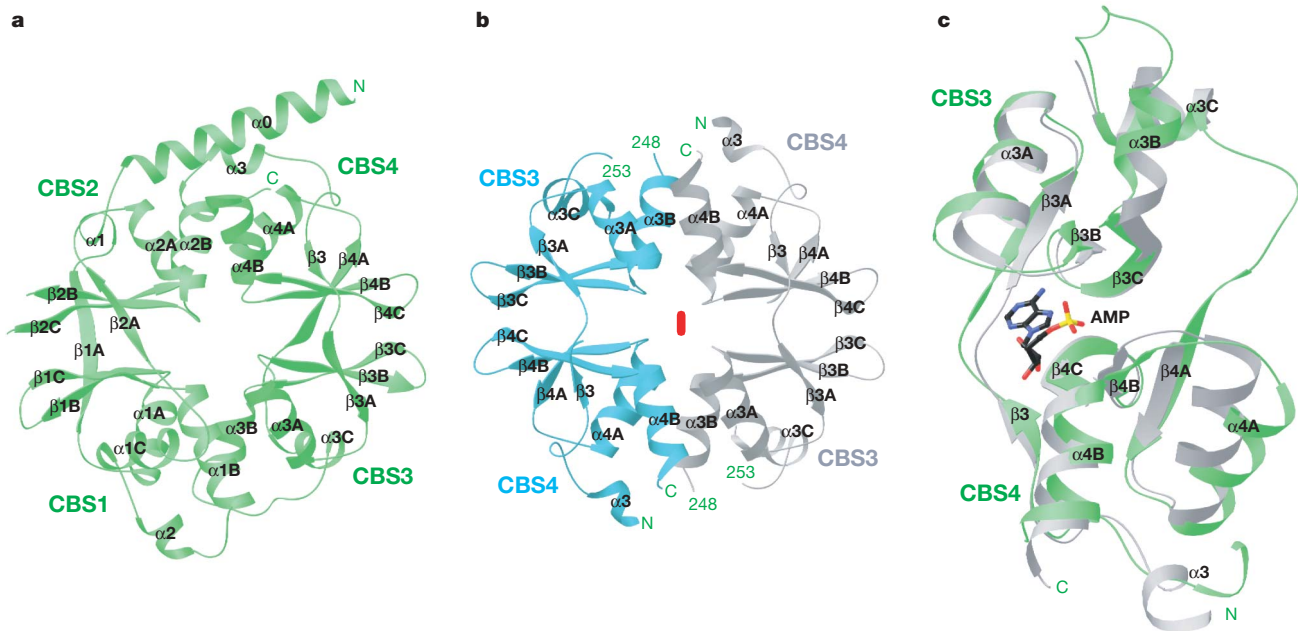


Figure 2 | Large conformational differences for the Bateman2 domain of Snf4. **a**, Structure of the Snf4 subunit, consisting of a Bateman1:Bateman2 'heterodimer'. The secondary structure elements are named in accordance with the system devised earlier²⁶. **b**, Structure of the Bateman2-domain

dimer of Snf4 (ref. 26). The two monomers are arranged in a head-to-tail fashion. **c**, Overlay of the structures of the Bateman2 domain in full-length Snf4 (in green) and in the homodimer (in grey). Produced with Ribbons³⁰.

side chain of Arg 143 is disordered in this complex, and the phosphate group does not seem to have many strong interactions with Snf4. It remains to be determined whether the binding of AMP to Snf4 occurs in solution and why this binding does not seem to affect the activity of the SNF1 heterotrimer.

The *S. pombe* enzyme has been reported to be a dimer in the crystal and in solution⁹. Our crystal of the *S. cerevisiae* enzyme also contains a dimer, although the mode of dimerization is different from that of the *S. pombe* enzyme (Supplementary Fig. 8). The buried surface area for this dimeric association is relatively small, only about 600 Å² per monomer. The heterotrimer is probably monomeric in solution, which is consistent with our gel-filtration data.

Our structure of the SNF1 heterotrimer core has significant implications for the regulation of the protein kinase activity of this enzyme. Previous studies suggested that residues 381–518 of Snf1 represent a regulatory sequence^{15,18}. Residues 313–335 in the α 1-subunit of mammalian AMPK (equivalent to residues 367–392 in Snf1; Supplementary Fig. 1) may auto-inhibit the protein kinase domain, although additional regions also contribute to the regulation^{16,19}. The biochemical data show that the regulatory sequence may control both the inhibition and the activation of SNF1. It interacts with and inhibits the protein kinase domain in the inactive form of AMPK/SNF1, perhaps by binding in the active site groove (Supplementary Fig. 9) or by interacting with the small lobe of the

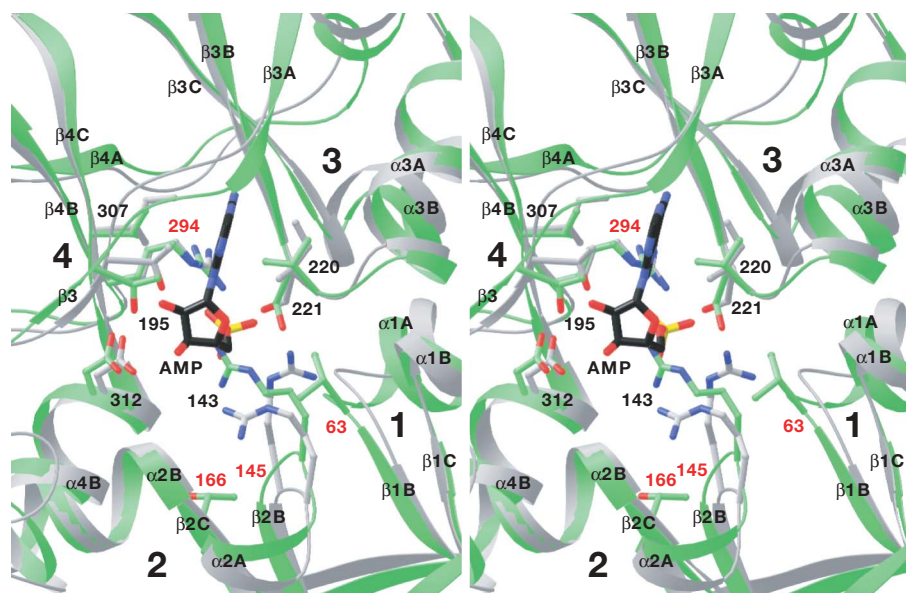


Figure 3 | Structure of the ligand-binding site in *S. cerevisiae* Snf4. Stereo-view overlay of the structures of the γ -subunits of *S. cerevisiae* SNF1 (Snf4, in green) and *S. pombe* AMPK (in grey)⁹. The position of AMP is observed in the *S. pombe* structure⁹, as well as from our studies. Residues that could

interact with AMP are shown, and those that are equivalent to disease-causing mutations in mammalian γ -subunits are labelled in red. Produced with Ribbons³⁰.

protein kinase domain¹⁹. On activation, the regulatory sequence establishes strong interactions with Snf4, thereby relieving the inhibition on the protein kinase domain¹⁵. A simple model based on our structure that is consistent with these data is shown in Supplementary Fig. 9.

Our structure reveals that residues 465–495 in the regulatory sequence are sequestered by Snf4 (Fig. 1b and Supplementary Fig. 6), indicating that this structure might correspond to the heterotrimer core of activated SNF1 (Supplementary Fig. 9). Further support for the importance of this interaction comes from the observation that one of the disease-causing mutations in the γ 2-subunit of mammalian AMPK, namely N488I (equivalent to Asn 251 in Snf4; Supplementary Fig. 3), is located near this part of the regulatory sequence (Fig. 1b). Mammalian AMPKs might therefore use a similar regulatory mechanism, although their sequences in this region are poorly conserved in comparison with Snf1 (Supplementary Fig. 1). Residues 496–518 of the regulatory sequence in Snf1 were found to be required for interaction with the protein kinase domain but not with Snf4 (ref. 15), which is consistent with our structural observations (Fig. 1b). It remains to be determined how the regulatory sequence is recognized by the protein kinase domain in the inactive form of SNF1/AMPK, and how the binding of different ligands to the γ -subunit can control its interaction with the regulatory sequence (Supplementary Fig. 9). Our structure shows that the AMP-binding site and the regulatory sequence are located on opposite faces of the Snf4 disc (Fig. 1b). Our structural information will also be helpful in characterizing, at the molecular level, other mechanisms for the regulation of this heterotrimeric enzyme^{1–4,6,29}.

METHODS SUMMARY

S. cerevisiae Snf1 (residues 398–633), Sip2 (residues 154–415) and Snf4 (residues 1–322) were expressed together by using a tri-cistronic expression system in the pET28a vector (Novagen) (Fig. 1a). The soluble protein was purified by Ni²⁺-affinity and gel-filtration chromatography. The protein was concentrated to 15 mg ml⁻¹ in a solution containing 50 mM Tris-HCl pH 8.5, 150 mM NaCl, 5 mM dithiothreitol and 5% (v/v) glycerol, and then stored at -80 °C.

Crystals of the heterotrimeric complex were obtained by the hanging-drop vapour-diffusion method at 21 °C. The reservoir solution contained 250 mM ammonium citrate pH 7.0 and 15% (w/v) PEG3350. The protein solution was supplemented with 1 mM AMP. The crystals belong to space group C2, with unit cell parameters of $a = 112.3 \text{ \AA}$, $b = 81.8 \text{ \AA}$, $c = 174.7 \text{ \AA}$ and $\beta = 102.2^\circ$. There are two copies of the heterotrimer in the crystallographic asymmetric unit. X-ray diffraction data were collected at the X29A beamline of the National Synchrotron Light Source (NSLS). The data processing statistics are summarized in Supplementary Table 1.

The structure was solved by the molecular replacement method, using the structures of the *S. pombe* heterotrimer⁹ as well as the GBD of the rat β 1-subunit¹⁰ as the models. After structure refinement, the models were modified to fit the electron density and sequence of *S. cerevisiae* SNF1, and additional residues that were not in the search models were located. The refinement statistics are summarized in Supplementary Table 1.

Full Methods and any associated references are available in the online version of the paper at www.nature.com/nature.

Received 15 May; accepted 27 July 2007.

Published online 12 September 2007.

1. Kahn, B. B., Alquier, T., Carling, D. & Hardie, D. G. AMP-activated protein kinase: ancient energy gauge provides clues to modern understanding of metabolism. *Cell Metab.* **1**, 15–25 (2005).
2. Hardie, D. G. & Sakamoto, K. AMPK: a key sensor of fuel and energy status in skeletal muscle. *Physiology* **21**, 48–60 (2006).
3. Carling, D. AMP-activated protein kinase: balancing the scales. *Biochimie* **87**, 87–91 (2005).
4. Kemp, B. E. *et al.* AMP-activated protein kinase, super metabolic regulator. *Biochem. Soc. Trans.* **31**, 162–168 (2003).

5. Viollet, B. *et al.* Physiological role of AMP-activated protein kinase (AMPK): insights from knockout mouse models. *Biochem. Soc. Trans.* **31**, 216–219 (2003).
6. Hardie, D. G., Carling, D. & Carlson, M. The AMP-activated/SNF1 protein kinase subfamily: metabolic sensors of the eukaryotic cell? *Annu. Rev. Biochem.* **67**, 821–855 (1998).
7. Hong, S.-P. & Carlson, M. Regulation of Snf1 protein kinase in response to environmental stress. *J. Biol. Chem.* **282**, 16838–16845 (2007).
8. Sanz, P. Snf1 protein kinase: a key player in the response to cellular stress in yeast. *Biochem. Soc. Trans.* **31**, 178–181 (2003).
9. Townley, R. & Shapiro, L. Crystal structures of the adenylate sensor from fission yeast AMP-activated protein kinase. *Science* **315**, 1726–1729 (2007).
10. Polekhina, G. *et al.* Structural basis for glycogen recognition by AMP-activated protein kinase. *Structure* **13**, 1453–1462 (2005).
11. Polekhina, G. *et al.* AMPK β subunit targets metabolic stress sensing to glycogen. *Curr. Biol.* **13**, 867–871 (2003).
12. Wiatrowski, H. A. *et al.* Mutations in the Gal83 glycogen-binding domain activate the Snf1/Gal83 kinase pathway by a glycogen-independent mechanism. *Mol. Cell. Biol.* **24**, 352–361 (2004).
13. Hudson, E. R. *et al.* A novel domain in AMP-activated protein kinase causes glycogen storage bodies similar to those seen in hereditary cardiac arrhythmias. *Curr. Biol.* **13**, 861–866 (2003).
14. Iseli, T. J. *et al.* AMP-activated protein kinase β subunit tethers α and γ subunits via its C-terminal sequence (186–270). *J. Biol. Chem.* **280**, 13395–13400 (2005).
15. Jiang, R. & Carlson, M. Glucose regulates protein interactions within the yeast SNF1 protein kinase complex. *Genes Dev.* **10**, 3105–3115 (1996).
16. Crute, B. E., Seefeld, K., Gamble, J., Kemp, B. E. & Witters, L. A. Functional domains of the α 1 catalytic subunit of the AMP-activated protein kinase. *J. Biol. Chem.* **273**, 35347–35354 (1998).
17. Jiang, R. & Carlson, M. The Snf1 protein kinase and its activating subunit, Snf4, interact with distinct domains of the Sip1/Sip2/Gal83 component in the kinase complex. *Mol. Cell. Biol.* **17**, 2099–2106 (1997).
18. Leech, A., Nath, N., McCartney, R. R. & Schmidt, M. C. Isolation of mutations in the catalytic domain of the Snf1 kinase that render its activity independent of the Snf4 subunit. *Eukaryot. Cell* **2**, 265–273 (2003).
19. Pang, T. *et al.* Conserved α -helix acts as autoinhibitory sequence in AMP-activated protein kinase α subunits. *J. Biol. Chem.* **282**, 495–506 (2007).
20. Rudolph, M. J., Amodeo, G. A., Bai, Y. & Tong, L. Crystal structure of the protein kinase domain of yeast AMP-activated protein kinase Snf1. *Biochem. Biophys. Res. Commun.* **337**, 1224–1228 (2005).
21. Nayak, V. *et al.* Structure and dimerization of the kinase domain from yeast Snf1, a member of the Snf1/AMPK protein family. *Structure* **14**, 477–485 (2006).
22. Bateman, A. The structure of a domain common to archaeobacteria and the homocystinuria disease protein. *Trends Biochem. Sci.* **22**, 12–13 (1997).
23. Kemp, B. E. Bateman domains and adenosine derivatives form a binding contract. *J. Clin. Invest.* **113**, 182–184 (2004).
24. Scott, J. W. *et al.* CBS domains form energy-sensing modules whose binding of adenosine ligands is disrupted by disease mutations. *J. Clin. Invest.* **113**, 274–284 (2004).
25. Hamilton, S. R. *et al.* An activating mutation in the γ 1 subunit of the AMP-activated protein kinase. *FEBS Lett.* **500**, 163–168 (2001).
26. Rudolph, M. J. *et al.* Structure of the Bateman2 domain of yeast Snf4: dimeric association and relevance for AMP binding. *Structure* **15**, 65–74 (2007).
27. Day, P. *et al.* Structure of a CBS-domain pair from the regulatory γ 1 subunit of human AMPK in complex with AMP and ZMP. *Acta Crystallogr. D* **63**, 587–596 (2007).
28. Adams, J. *et al.* Intrasteric control of AMPK via the γ 1 subunit AMP allosteric regulatory site. *Protein Sci.* **13**, 155–165 (2004).
29. Sanders, M. J., Grondin, P. O., Hegarty, B. D., Snowden, M. A. & Carling, D. Investigating the mechanism for AMP activation of the AMP-activated protein kinase cascade. *Biochem. J.* **403**, 139–148 (2007).
30. Carson, M. Ribbon models of macromolecules. *J. Mol. Graph.* **5**, 103–106 (1987).

Supplementary Information is linked to the online version of the paper at www.nature.com/nature.

Acknowledgements We thank M. Carlson for helpful discussions; H. Robinson and N. Whalen for setting up the X29A beamline; and J. Schwanof and R. Abramowitz for setting up the X4C beamline at the National Synchrotron Light Source. This research is supported in part by an NIH grant to L.T. G.A.A. was supported by an NIH training program in molecular biophysics.

Author Information The atomic coordinates are deposited at the Protein Data Bank under accession number 2QLV. Reprints and permissions information is available at www.nature.com/reprints. The authors declare no competing financial interests. Correspondence and requests for materials should be addressed to L.T. (ltong@columbia.edu).

METHODS

Protein expression and purification. The three subunits of *S. cerevisiae* SNF1 (residues 398–633 of Snf1, residues 154–415 of Sip2 and residues 1–322 of Snf4) were expressed together using a polycistronic expression system in the pET28a vector (Novagen) (Fig. 1a). The boundaries of each subunit were defined by sequence and secondary structure analysis as well as by experimental sampling of different start sites for the Snf1 and Sip2 subunits. Sip2 carried an N-terminal hexahistidine tag. The proteins were overexpressed in *E. coli* BL21 (DE3) Rosetta cells at 20 °C and purified by Ni²⁺-affinity and gel-filtration chromatography. The protein was concentrated to 15 mg ml⁻¹ in a buffer containing 50 mM Tris-HCl pH 8.5, 150 mM NaCl, 5 mM dithiothreitol and 5% (v/v) glycerol. The protein sample was divided into small aliquots, flash-frozen in liquid nitrogen and then stored at -80 °C. The N-terminal hexahistidine tag was not removed for crystallization. SDS gel electrophoresis on the purified protein showed that the three subunits are present at roughly equal molar concentrations (Supplementary Fig. 1b).

The selenomethionyl protein was produced by using a methionine auxotroph in the defined LeMaster medium³¹, and purified by following the same protocol as that for the native protein.

Protein crystallization. Crystals of the *S. cerevisiae* SNF1 heterotrimer core were obtained by the hanging-drop vapour diffusion method at 21 °C. The reservoir solution contained 250 mM ammonium citrate pH 7.0 and 15% (w/v) PEG3350, and 1 mM AMP was included in the protein solution. Micro-seeding was crucial for producing crystals of sufficient size for structural studies. The crystals were cryoprotected in the reservoir solution supplemented with 12.5% (w/v) PEG3350, and flash-frozen in liquid nitrogen for data collection at 100 K. The crystals belong to space group C2, and the unit cell parameters of the crystal used for data collection are $a = 112.3 \text{ \AA}$, $b = 81.8 \text{ \AA}$, $c = 174.7 \text{ \AA}$, and $\beta = 102.2^\circ$. There are two copies of the SNF1 heterotrimer core in the crystallographic asymmetric unit.

Data collection and processing. A native data set to 2.6 Å resolution and a selenomethionyl single-wavelength anomalous diffraction (SAD) data set to 3.5 Å resolution were collected on an ADSC CCD at the X29A beamline of the National Synchrotron Light Source (NSLS). The diffraction images were processed and scaled with the HKL package³². The data processing statistics are given in Supplementary Table 1.

Structure determination and refinement. The structure of SNF1 heterotrimer core was solved by the molecular replacement method with the program Phaser³³. The structures of the *S. pombe* heterotrimer³⁴ as well as the GBD of the rat β1-subunit³⁵ were used as the models. The structure refinement was performed with the programs CNS³⁶ and Refmac³⁷. The models were manually modified to fit the electron density as well as the sequence of *S. cerevisiae* SNF1,

using the programs O³⁸ and Coot³⁹. Additional residues that were not in the search models were also located. Non-crystallographic symmetry restraints were applied at the beginning stages of the refinement, but were released in the later stages with only minor effects on the *R* and free *R* values. The correctness of the structure solution was confirmed by anomalous difference electron density maps calculated based on the selenomethionyl SAD data. The refinement statistics are presented in Supplementary Table 1.

Observation of AMP binding to the SNF1 heterotrimer. Crystals were obtained by the hanging-drop vapour diffusion method at 21 °C. The reservoir solution contained 210 mM ammonium citrate pH 7.0 and 20% (w/v) PEG3350. The protein solution was supplemented with 1 mM AMP. Micro-seeding was crucial for producing crystals of sufficient size for structural studies. The crystals were cryoprotected in the reservoir solution supplemented with 20% (w/v) PEG3350 as well as 10 mM glucose 6-phosphate for about 16 h, and flash-frozen in liquid nitrogen for data collection at 100 K. The crystals belong to space group C2, with unit cell parameters of $a = 124.2 \text{ \AA}$, $b = 74.7 \text{ \AA}$, $c = 195.4 \text{ \AA}$, and $\beta = 107.4^\circ$. There are two copies of the heterotrimer in the crystallographic asymmetric unit. An X-ray diffraction data set to 3.3 Å resolution was collected at the X4C beamline of the NSLS. The structure was solved by molecular replacement. After crystallographic refinement in the absence of any ligand, the $2F_o - F_c$ electron density seems consistent with the presence of AMP.

- Hendrickson, W. A., Horton, J. R. & LeMaster, D. M. Selenomethionyl proteins produced for analysis by multiwavelength anomalous diffraction (MAD): a vehicle for direct determination of three-dimensional structure. *EMBO J.* **9**, 1665–1672 (1990).
- Otwinowski, Z. & Minor, W. Processing of X-ray diffraction data collected in oscillation mode. *Methods Enzymol.* **276**, 307–326 (1997).
- Storoni, L. C., McCoy, A. J. & Read, R. J. Likelihood-enhanced fast rotation functions. *Acta Crystallogr. D* **60**, 432–438 (2004).
- Townley, R. & Shapiro, L. Crystal structures of the adenylate sensor from fission yeast AMP-activated protein kinase. *Science* **315**, 1726–1729 (2007).
- Polekhina, G. *et al.* Structural basis for glycogen recognition by AMP-activated protein kinase. *Structure* **13**, 1453–1462 (2005).
- Brunger, A. T. *et al.* Crystallography & NMR System: A new software suite for macromolecular structure determination. *Acta Crystallogr. D* **54**, 905–921 (1998).
- Murshudov, G. N., Vagin, A. A. & Dodson, E. J. Refinement of macromolecular structures by the maximum-likelihood method. *Acta Crystallogr. D* **53**, 240–255 (1997).
- Jones, T. A., Zou, J. Y., Cowan, S. W. & Kjeldgaard, M. Improved methods for building protein models in electron density maps and the location of errors in these models. *Acta Crystallogr. A* **47**, 110–119 (1991).
- Emsley, P. & Cowtan, K. D. Coot: model-building tools for molecular graphics. *Acta Crystallogr. D* **60**, 2126–2132 (2004).